Einfluss des Bildrauschens innerhalb der Messkette eines industriellen Computertomografen - Propagation of image noise through the measurement chain in industrial X-ray computed tomography

Tamara REUTER [1], Andreas Michael MÜLLER [1], Tino HAUSOTTE [1]
[1] Friedrich-Alexander-Universität Erlangen-Nürnberg (FAU), Lehrstuhl für Fertigungsmesstechnik (FMT), Erlangen

Contact E-Mail: tamara.reuter@fmt.fau.de

Abstract. Industrial X-ray computed tomography is a technology that is able to measure inner and outer features at once. This fact leads to an increasing interest for the application in the context of dimensional metrology. In order to evaluate the quality of a measurement, the task specific measurement uncertainty has to be determined. Currently, VDI/VDE 2630 part 2.1 gives a guideline to determine the task specific measurement uncertainty with a large number of experimental repetitions and a calibrated workpiece. Thus, current research aims to determine this measurement uncertainty numerically using simulations. To achieve this, all relevant factors influencing a measurement and their impact on the specific measurand have to be investigated.

One of these influencing factors is the image noise originating from different sources within the measurement chain. In this contribution, we will analyse how different noise levels, given as signal-to-noise ratios (SNR) at the maximum intensity of a free beam, will influence the measured geometry of a scanned part. The local statistical behaviour of the measured surface is determined from measurement repetitions (simulations with aRTist 2.12 (BAM, Berlin)), followed by a dense geometric sampling of each surface, using the discrete uncertainty framework developed at FMT. This method allows us to make locally resolved statements about the measurement uncertainty at arbitrary surface points without the need for specific dimensional measurands and is therefore well suited for the evaluation of the propagation of projection noise through the complete measurement chain.

Introduction

X-ray computed tomography (CT) is an imaging technique that is based on the measurement of the interaction of radiation with matter [1]. Because it is able to detect inner and outer features at once, this method is applied in non-destructive testing and in dimensional metrology [2]. For an accurate and reliable measurement, the traceability to the meter (SI unit of length) is an important key factor. To achieve this, the determination of the task-

specific measurement uncertainty is essential [3]. Currently, one focus of research and of the corresponding industry is the evaluation and determination of the task-specific measurement uncertainty using simulation with the aim to apply this method in quality control for example in the automotive industry [4,5]. VDI/VDE 2630 part 2.1 gives a guideline to evaluate the task-specific measurement uncertainty by conducting repeated measurements of a calibrated workpiece with a CT system [6]. However, in times of industry 4.0 and thus digitalisation, the determination of the measurement uncertainty is aimed to be done by simulation as it is time and cost effective. The guideline mentioned above describes the implementation of the substitution method for CT measurements. The radiographic simulation can be used as one solution for this substitution [6,7]. To achieve the application of simulation as a tool for evaluating the measurement uncertainty, all influencing factors to a CT measurement and their impact on the measurands have to be determined and evaluated [6].
Image noise is a well-known factor that has to be considered when determining the measurement uncertainty [4]. According to [4] most research focuses on the topic of how noise can be measured and how noise can be reduced (e.g. see [8–10]). However, some studies have investigated in a first step to what extent noise contributes to the measurement uncertainty. Müller et al. [11] investigated the influence of noise and resolution to dimensional measurements. Matern [12] as well as Hiller and Kasperl [13] discussed the influence of projection noise on dimensional measurands.
With this contribution we want to investigate how different projection noise levels influence individual surface points through a complete measurement chain of a dimensional measurement with a virtual copy of the CT system (used at the FMT) using the discrete uncertainty framework developed at FMT. We also want to show to what extent the discrete uncertainty of the surfaces of the simulated volumes deviate from the discrete uncertainty of the surface of the volume measured with a comparable real CT system.

1. Method and Material

For this simulative study we varied both the signal-to-noise ratio (SNR) and the material of the test specimen respectively. The SNR is given as a SNR_{max} to the simulation software at the free-beam maximum grey level intensity (I_{max} = 60000, resolution 16 bit) at the detector. The local SNR for each pixel scales according to [1] with the square root of the intensity. This method was used as the intensity reaching the detector is not homogenously distributed over each pixel for a cone beam CT. This implementation is typically for image noise [14] and leads to a root-shaped curve without any additional constant noise factors. Figure 1 illustrates three possible ways to implement the SNR with regard to the increasing energy density. The implementation of a realistic SNR curvature is difficult, as different noise factors, like electrical noise or thermal noise have to be considered as well and leads thus to different curvatures.

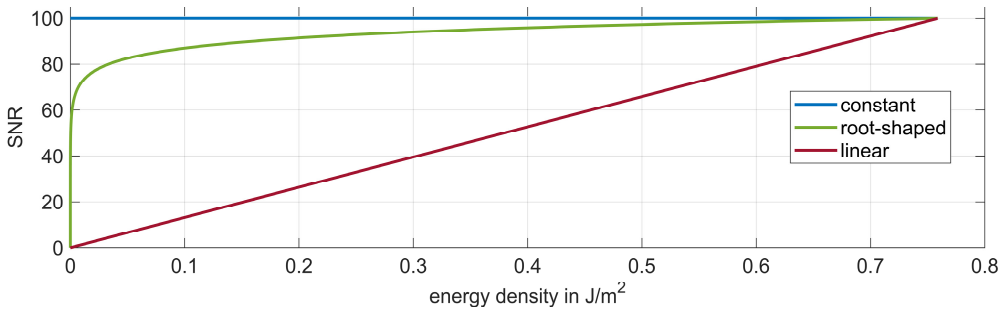

Figure 1: Schematic illustration of different approaches to implement a SNR_{max} 100 to a simulation software with regard to the energy density.

The power of the tube, the integration time and the detector response were arranged such that the grey values reach a maximum of 60000 at a free beam. We simulated nine different scenarios (3 different materials with 3 different SNR_{max}) and each scenario was repeatedly measured 20 times. Every random generator of each simulation was initialised with a different start value, so that the simulated grey value variations of each simulation are different.
The parameters of the simulated CT system were leaned on the CT system Zeiss Metrotom 1500, available at FMT, so that we get a first idea to what extent we are able to simulate a realistic CT scan. Table 1 gives an overview of the used parameters.

Table 1: Parameters used for the simulations

Geometry		Detector	
Source-Detector Distance (SDD)	1375 mm	Size	2048 px x 2048 px
Source-Object Distance (SOD)	270 mm	Pixel size	0.200 mm x 0.200 mm
		Projection noise	SNR at I_{max}: 100, 300, 500
Test specimen:	Multi-feature specimen	Source	
Material	Aluminium (Al, ρ = 2.6989 g/cm^3), Titan (Ti, ρ = 4.5 g/cm^3), Plastics (PE, ρ = 0.95 g/cm^3)	Polychromatic X-ray spectrum	Al: 140 kVp / 60 µA, Ti: 200 kVp / 180 µA, PE: 100 kVp / 720 µA
		Pre-filter	Cu: 0.25 mm
		Spot-type	Gaussian distributed with σ = 48.9 µm

Figure 2 shows the test specimen that we used for our investigation and a schematic image of the scenery.

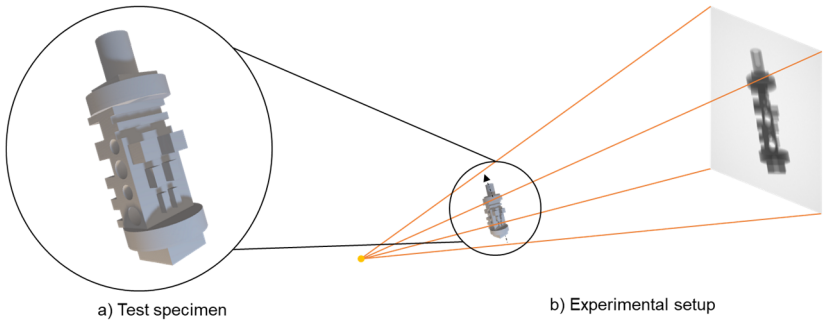

Figure 2: a) Test specimen and b) scenery of the experiments

Every scenario was formulated in a general description framework, the JSON file format (JavaScript Object Notation), with which a full CT scan can be described. This secures the reproducibility of the investigations and has the advantage to have a scenario description in a human-readable and writable as well as a machine-readable and writeable format [15]. The simulations were then carried out with the CT simulator aRTist 2.12 using a special parser, which was developed for this file format. The flat field correction of the projections was done with the CTSimU software toolbox [16] and the subsequent CT reconstruction of the simulated scan was carried out with the software CERA 6.1.1 (Siemens Healthcare GmbH),

using standard FDK reconstruction. The surface determination was done with VGStudio Max 3.5 (VGS) (Volume Graphics GmbH) using the ISO-50 local adaptive method. The measurements were exported as triangles meshes (STL file format) using the "precise with simplification" setting in VGS.

2. Determination of the discrete uncertainty of a surface from repeated measurements

Instead of evaluating dimensional measurands (e.g., based on Geometrical Product Specification, GPS), the measurement uncertainty is determined for discrete surface points with respect to the nominal geometry. Using a simulation environment offers the great advantage, that systematic measurement errors can be calculated by comparison of the measurement results with the nominal geometry, because the geometry of the object is part of the input parameters into the simulation and therefore known beforehand. Of course, this does not apply for real world measurements, due to deviations introduced by manufacturing. Additionally, the relationship between the coordinate system of the input geometry and the measurement system, respectively, is well known, because the placement of the measurement object inside the measurement volume of the CT is part of the simulation input parameters. The discrete measurement uncertainty determination[1] follows these main steps:

I. Convert the CAD model of the measurement object (STEP file format) into a triangle mesh (STL file format), using commercial software (e.g., Inventor 2020). Use this STL geometry as input parameter for the simulated measurements, such that each input parameter combination (3x SNR, 3x material, see Table 1) is repeatedly measured 20 times, resulting in 180 single measurements.

II. Alter the input triangle mesh, such that a homogeneous distribution of triangle edge points represents its geometry. These points are called discrete (hence the name) sampling points (SP) and each SP lies exactly on the original mesh (the represented geometry remains perfectly identical at SP locations, only its structure is altered). We created[2] such a mesh offering a mean triangle edge length of 50 µm (Gaussian distributed, approx. 6 million triangles).

III. Align the measurements with the nominal geometry. As mentioned above, within a simulation environment, this step is trivial, but for real measurements, additional effort is required by means of a registration routine.

IV. Considering a measurement series consisting of 20 single measurements, determine the 20 closest hit locations (HL) from each SP to each single measurement searching in both directions of the vertex normal vector of SP. In other words, shoot a ray from each SP in both directions of its vertex vector and find the closest intersection with each targeted surface. Thus, each SP is now associated with 20 HL, from which 20 (signed[3]) distance values D can be computed. These intersection tests were performed using GPU acceleration based on the parallel programming model CUDA.

V. For each SP, calculate the systematic and random measurement errors, M_{sys} and M_{rnd}, as the mean value and the standard deviation of D, respectively. The expanded measurement uncertainty associated with each SP is

$$U_{\mathrm{exp}} = k\sqrt{{M_{\mathrm{rnd}}}^2 + {M_{\mathrm{sys}}}^2},$$

using $k = 2$.

[1] Related publications describing the method in more detail can be found [17–19].
[2] Using own software in combination with the 3D Delaunay Triangulator TetGen [20].
[3] The sign is dependent on the normal vector of SP.

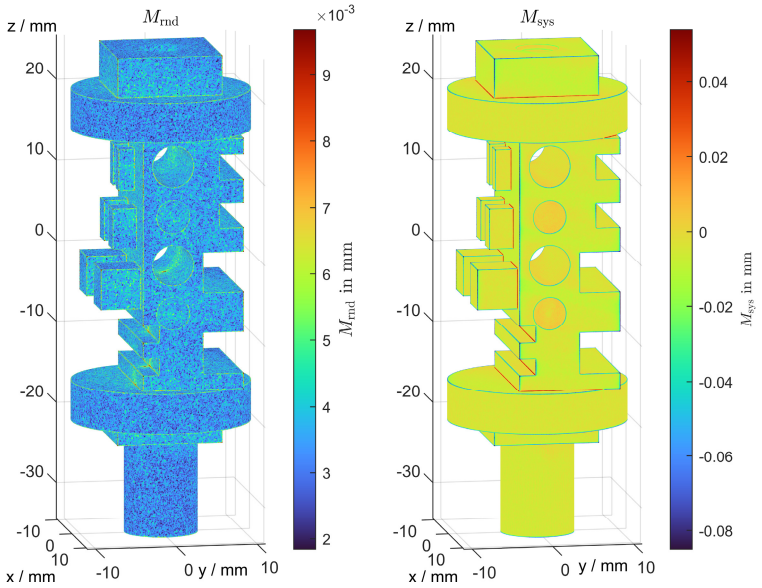

Figure 3: Visualisation of the random measurement error M_{rnd} (left) and the systematic measurement error M_{sys} (right) from 20 repeated measurements of "Al-100". Colour map limits are the upper/lower 0.1 percentiles.

An example showing M_{rnd} and M_{sys} for the configuration Material Aluminium and SNR 100 ("Al-100") is given in Figure 3. As expected, sharp edges are rounded, leading to systematic measurement errors. The random measurement error is mostly homogeneously distributed over the complete surface.

3. Evaluation of results

In the following, statistical evaluations are used to compare the 9 different measurement series. Furthermore, a "real" measurement series consisting of 20 measurement repetitions of the manufactured object (Aluminium) was added (Zeiss Metrotom 1500, VAST scan, 1000 ms integration time, 2050 projections, 150 kVp). This measurement was compared against a CMM (Coordinate Measurement Machine) reference measurement (Zeiss UPMC), which was converted into a triangle mesh [21]. The coordinate transformation (registration) aligning this measurement series with the associated CMM reference measurement was performed considering all measurements at once (instead of individual registration) using own registration algorithms[4]. The following figures show normalised histograms as cumulative density function estimates. Thus, the x-value at $y = 0.5$ corresponds to the median value of a curve. The curves are cut at their 2.5 and 97.5 percentile, respectively, in order to increase clarity. Solid lines refer to the highest SNR (500), followed by dashed lines (lower SNR - 300) and dotted lines (lowest SNR - 100).

[4] This prevents the compensation of measurement drifts (which are therefore regarded as part in the observed uncertainty) by the registration routine and can also reduce the method uncertainty of the registration algorithm.

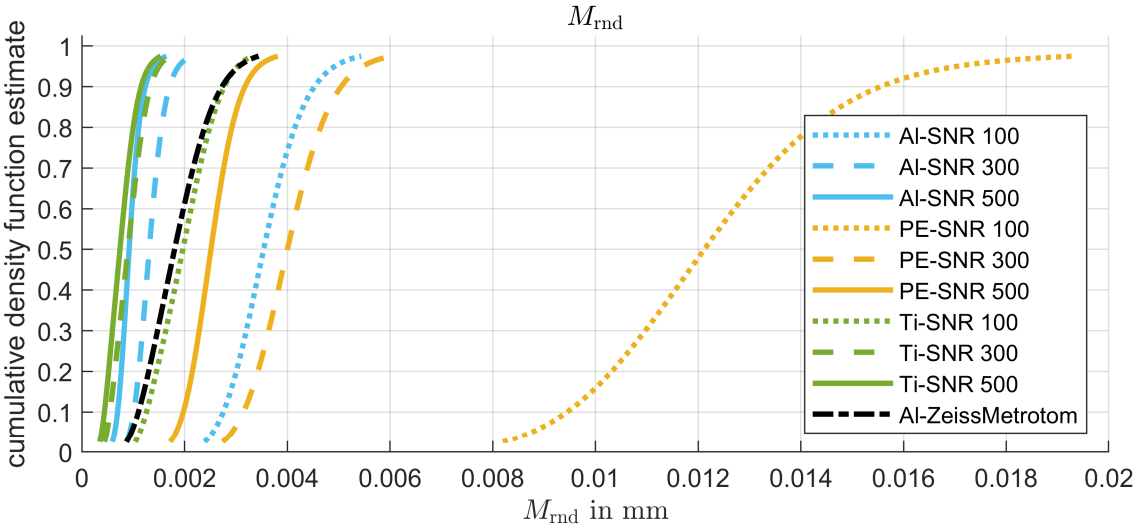

Figure 4: Comparison of the random measurement errors M_{rnd} for all SP showing 10 measurement series. Lower SNR values consistently increase the observed M_{rnd}. Additionally, lower M_{rnd} are observed for more dense materials. The results of the real measurement series lie in between the results of the virtual measurement series with Al SNR 100 and 300.

The cumulative density functions for the random measurement errors M_{rnd} (absolute values) are presented in Figure 4. As expected, lower SNR values consistently increase the observed M_{rnd}, as the image noise increases with lower SNR. More dense materials create higher contrasts in the volume data and thus a better contrast-to-noise ratio (CNR). Therefore, the M_{rnd} decreases with increasing density. Importantly in that context, the used virtual detector does not require an optimal intensity window, in which it behaves linearly. The values for the "real" measurement series lie in between the results of the virtual measurement series with Al-SNR 100 and 300, but closer to the results of the Al-SNR 300.

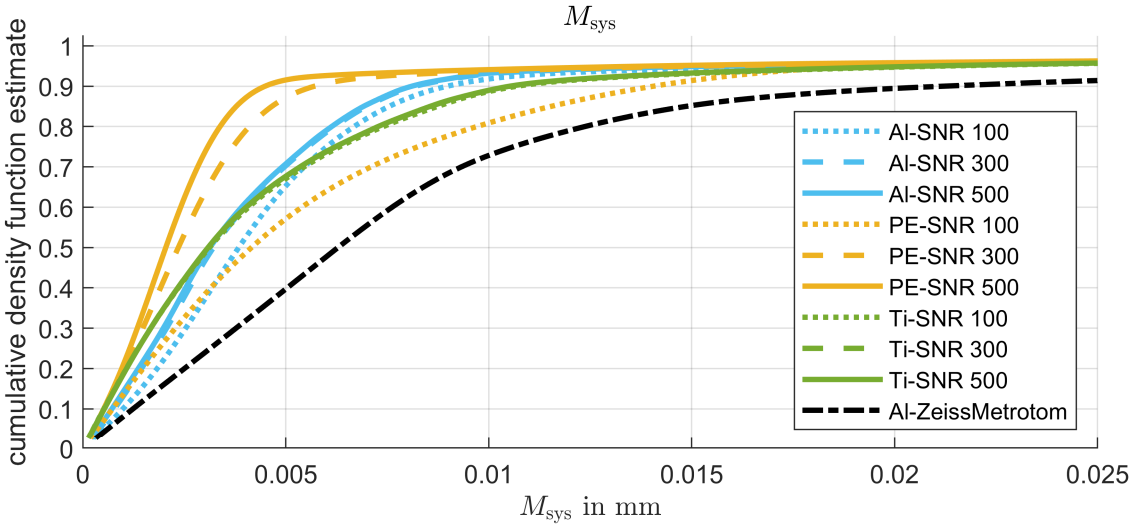

Figure 5: Comparison of the systematic measurement error M_{sys} for all SP showing 9 virtual measurement series and 1 real measurement series. Lower SNR values lead to increasing M_{sys}. However, M_{sys} behaves invariant with respect to the SNR for the Ti series.

Figure 5 shows the cumulative density functions for the systematic measurement errors (absolute values). As already seen for the M_{rnd}, the lower the SNR the higher the M_{sys}. However, M_{sys} behaves invariantly for the measurements with Ti with nearly the same systematic measurement error. One possible explanation of this behaviour could be the density of this material and thus the higher achievable contrast in comparison to PE or Al. A second assumption for this behaviour is due to the implementation of the SNR, as a free-beam $\mathrm{SNR}_{\mathrm{max}}$ at I_{max}. This leads to the fact, that the SNR has less effect to simulations with Ti than with PE. The "real" measurement series shows the highest M_{sys} and has a higher M_{sys}

compared to the counterpart virtual measurements. This difference can be explained due to a high difference in the virtual copy of the CT system and the simulation of the SNR. In case of the virtual measurements only the image noise is simulated. Within the real CT system more factors influence the measurement. The expanded measurement uncertainty increases with lower SNR and lower material density as illustrated in Figure 6. The highest difference between the test series of one material is seen for PE. The test series for Ti has nearly no difference between the different SNRs. The measurement series "Al-ZeissMetrotom" conducted with a real test specimen made of Al shows the smallest incline but the highest uncertainty. This is mainly due to the higher systematic measurement error.

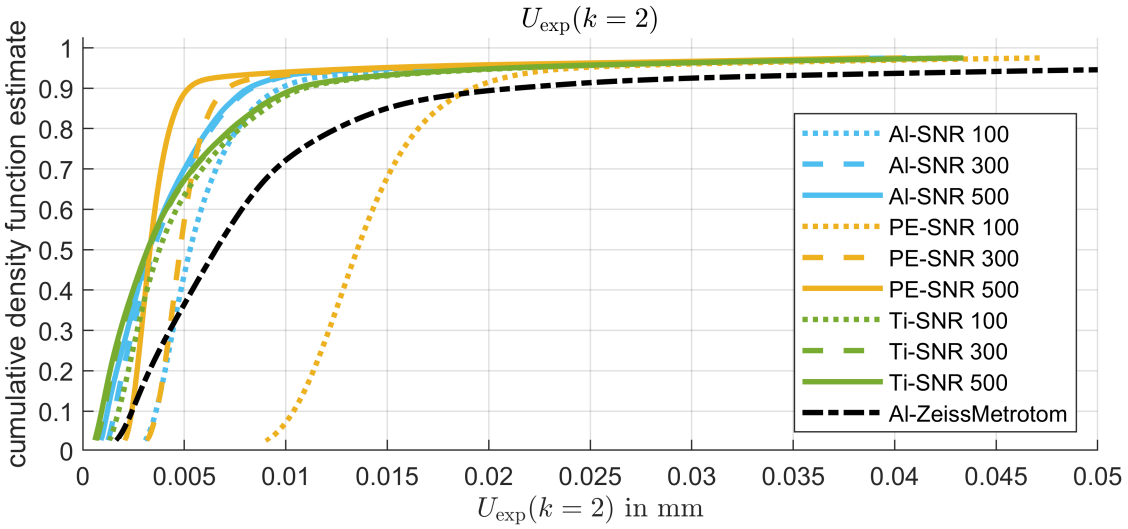

Figure 6: Comparison of the expanded measurement uncertainty U_{exp} for all SP showing 9 virtual measurement series and 1 real measurement series. Lowe SNR leads to increasing U_{exp}. The higher the density of the material the smaller is the deviation between the U_{exp} of the different SNR.

4. Summary and Outlook

With this contribution, we investigated the influence of image noise on simulated volumes. We therefore used the discrete uncertainty framework to investigate how the image noise influences the surface of the volumes in comparison to the nominal geometry. We therefore conducted a line of test scenarios with different SNRs and different materials of the test specimen. In order to compare our virtual test setup with a real CT system available at our institution, we also conducted one test series with the CT system Zeiss Metrotom and used the same test specimen made out of Al.

The results have shown that the random and systematic measurement errors of the discrete surface points increase as the SNR decreases, and thus the image noise increases. This behaviour is due to the fact, that with decreasing SNR the standard deviation of the simulated grey values of each pixel in the projections increases.

In case of the material Ti, indicate that all discrete surface points of volumes simulated with different SNRs have the same systematic measurement error. This fact can be described as the density of Ti leads to higher contrasts in the volume data and thus a better CNR.

The expanded measurement uncertainty for the 9 virtual measurement series, increases with decreasing SNR. The deviation between one test series of the same material, but deviating SNR, decreases with an increasing density of the material as the contrast on the projection increases. The results of the virtual measurement series have shown, that we are able to illustrate with the discrete uncertainty framework differences in the surfaces of the volumes when different image noise levels and material densities exist.

Comparing the results of the virtual measurements with Al and the test series with the CT system Zeiss Metrotom show that the virtual copy of the CT system deviates. This deviation can be explained through the implementation of the SNR and the idealised detector setup. In our implementation, we scaled the SNR with the square root of the intensity and included no other noise factors, like electrical noise, thermic noise or noise caused by the scintillator, as they exist in reality. Further research should therefore deal with a close to realistic implementation of the detector in the simulation and adding besides images noise, other noise factors as mentioned above.

Contributions according to CRediT [22]

Tino Hausotte (TH) contributed to funding acquisition and project administration, supervision and resources. Tamara Reuter (TR), Andreas Müller (AM) and TH contributed to the review and finalisation of the full paper. TR and AM contributed the conceptualisation, methodology, investigation, formal analysis, data curation, software, validation, visualisation and wrote the original draft.

Acknowledgements

The authors would like to thank the project CTSimU (WIPANO project 03TNH026A). WIPANO projects are financed by the German Federal Ministry for Economic Affairs and Energy and managed by Project Management Jülich.
The authors would like to thank the German Research Foundation (DFG) for supporting the research project “FOR 2271: process-oriented tolerance management based on virtual computer-aided engineering tools” under grant number HA 5915/9-2 and for the financial support of the acquisition of the CT system Zeiss Metrotom 1500 through Grant No. 324672600.
The authors would also like to thank Siemens Healthcare GmbH for providing the CT software CERA.

References

[1] T.M. Buzug, Computed tomography: From photon statistics to modern cone-beam CT with 10 tables, Springer, Berlin, Heidelberg, 2008.
[2] J.P. Kruth, M. Bartscher, S. Carmignato, R. Schmitt, L. de Chiffre, A. Weckenmann, Computed tomography for dimensional metrology, CIRP Annals 60 (2011) 821–842. https://doi.org/10.1016/j.cirp.2011.05.006.
[3] M. Bartscher, M. Neukamm, U. Hilpert, U. Neuschaefer-Rube, F. Härtig, K. Kniel, K. Ehrig, A. Staude, J. Goebbels, Achieving Traceability of Industrial Computed Tomography, KEM 437 (2010) 79–83. https://doi.org/10.4028/www.scientific.net/KEM.437.79.
[4] Á.R. Sánchez, A. Thompson, L. Körner, N. Brierley, R. Leach, Review of the influence of noise in X-ray computed tomography measurement uncertainty, Precision Engineering (2020).
[5] Durchstrahlungssimulation für die Messunsicherheitsbestimmung beim Messen geometrischer Merkmale mittels Röntgen-Computertomographie › Wipano - CTSimU. https://www.ctsimu.forschung.fau.de/ (accessed 23 March 2022).
[6] Verein Deutscher Ingenieure e.V., VDI/VDE 2630 Blatt 2.1, Düsseldorf, 2015.
[7] DIN CEN ISO/TS 15530-1, Geometrical product specifications (GPS) — coordinate measuring machines (CMM): technique for determining the uncertainty of

measurement — Part 3: use of calibrated workpieces or measurement standards (ISO: Geneva, Switzerland).
[8] A. Buratti, N. Grozmani, C. Voigtmann, L.V. Sartori, R.H. Schmitt, Determination of the optimal imaging parameters in industrial computed tomography for dimensional measurements on monomaterial workpieces, Measurement Science and Technology 29 (2018) 115009.
[9] O. Demirkaya, Reduction of noise and image artifacts in computed tomography by nonlinear filtration of projection images, 2001.
[10] T. Fuchs, S. Kasperl, L. Reindl, Einfluss der Bildqualität röntgentomographischer Abbildungen auf Koordinatenmessungen: Grundlagen, Messungen und Simulationen, 78 (2011) 334–347. https://doi.org/10.1524/teme.2011.0137.
[11] P. Müller, J. Hiller, A. Cantatore, M. Bartscher, L. De Chiffre, Investigation on the influence of image quality in X-ray CT metrology (2012).
[12] D. Matern, How much does image quality influence the form error in industrial X-Ray CT, 10th conference on industrial computed tomography (iCT), 2020, Wels, Austria.
[13] J. Hiller, S. Kasperl, Zum Verhältnis von Bildqualität und Messgenauigkeit in der CT-Metrologie, Industrielle Computertomografie Tagung, 2010, Wels, Austria.
[14] T. Reuter, D. Plotzki, F. Borges de Oliveira, T. Hausotte, Simulative Untersuchung des Einflusses von Bildrauschen auf dimensionelle Messungen mit industriellen Computertomografen, DGZfP-Jahrestagung 2021, Deutsche Gesellschaft für Zerstörungsfreie Prüfung e.V. (DGZfP), 2021.
[15] CTSimU Scenarios, 2021. https://bamresearch.github.io/ctsimu-scenarios/introduction.html (accessed 23 March 2022).
[16] CTSimU Software Toolbox, 2022. https://github.com/BAMresearch/ctsimu-toolbox (accessed 23 March 2022).
[17] A.M. Müller, D. Schubert, D. Drummer, T. Hausotte, Determination of the single point uncertainty of customized polymer gear wheels using structured-light scanning with various polygonization settings, J. Sens. Sens. Syst. 9 (2020) 51–60. https://doi.org/10.5194/jsss-9-51-2020.
[18] A.M. Müller, T. Hausotte, Analysis of the random measurement error of areal 3D coordinate measurements exclusively based on measurement repetitions, tm - Technisches Messen 88 (2021) 71–77. https://doi.org/10.1515/teme-2020-0087.
[19] A.M. Müller, T. Hausotte, Determination of the single point precision associated with tactile gear measurements in scanning mode, J. Sens. Sens. Syst. 9 (2020) 61–70. https://doi.org/10.5194/jsss-9-61-2020.
[20] H. Si, TetGen, a Delaunay-Based Quality Tetrahedral Mesh Generator, ACM Trans. Math. Softw. 41 (2015) 1–36. https://doi.org/10.1145/2629697.
[21] A.M. Müller, T. Hausotte, Improving template-based CT data evaluation by integrating CMM reference data into a CAD model-based high fidelity triangle mesh, Nondestructive Testing and Evaluation, accepted for publication, 2022.
[22] CASRAI, CRediT - Contributor Roles Taxonomy, 2020. https://casrai.org/credit/ (accessed 31 March 2022).